Lennart Carlsson

CYCLIC FATIGUE OF YTTRIA TETRAGONAL ZIRCONIA POLYCRYSTALS

SP Report 1990:02
Materials and Mechanics
Borås 1990

3H

ABSTRACT

Cyclic fatigue was studied for yttria tetragonal zirconia polycrystals in 4-point bending at room temperature. The number of cycles to failure decreased from $2 \cdot 10^6$ to 10^3 when the applied maximum stress was increased from 65 to 90 % of the flexure strength. Fractographic studies in the scanning electron microscope indicated that the catastrophic failure starts in accordance with the Griffith equation from a cyclically generated fatigued zone. X-ray diffraction investigations gave no evidence for differences on the amount of crystallographic changes from tetragonal to monoclinic phase in fracture surfaces for samples cyclically or monotonically loaded to failure.

Key words: Cyclic fatigue, yttria tetragonal zirconia polycrystals, four-point bending, fractography, scanning electron microscopy, X-ray diffraction.

STATENS PROVNINGSANSTALT

RAPPORT 1990:02
ISBN 91-7848-198-8
ISSN 0248-5172
Borås 1990

SWEDISH NATIONAL TESTING and RESEARCH INSTITUTE
Report 1990:02

Postal address:
P.O. Box 857, 501 15 Borås, Sweden
Telephone Int + 46 33 - 16 50 00
Telefax Int + 46 33 - 13 55 02
Telex 36252 Testing S

CONTENTS

SUMMARY

Ceramic materials have generally been presumed to be insensitive to degradation from cyclic fatigue at room temperature. It has frequently been suggested that there is no enhanced effect of cycling on crack propagation.

Cyclic fatigue was studied in four-point bending on yttria tetragonal zirconia polycrystals. The number of cycles to failure decreased from $2 \cdot 10^6$ to 10^3 cycles when the maximum stress was increased from 65 to 90% of the flexure strength.

Scanning electron microscopy revealed numerous intergranular micro-cracks in the fatigue zone near the origin of failure. Test bars monotonically loaded to failure showed fracture surfaces indicating transgranular fracture.

1 INTRODUCTION

The use of advanced ceramic materials rather than metallic materials for structural applications, such as in gas-turbine engines, has been motivated by their low density, far superior elevated-temperature strength and presumed insensitivity to degradation from cyclic fatigue [1]. Several recent reports, however, have given evidence for reduced lifetimes under cyclic loadings at stress levels clearly below the flexure strength.

The questioned existence of true cyclic crack propagation effects in ceramics has been based primarely on the very limited plasticity in these materials as opposed to dislocation-based periodic plastic deformation cycles in metals. Several mechanisms have been suggested as explanations for the fatigue effects in monolithic ceramics [2], but a quantitative model is still missing. Although a large number of papers have recently been presented, there is still a need for further experimental work.

This report presents results from cyclic, monotonic and static loadings of test bars of yttria tetragonal zirconia polycrystals (Y-TZP). The tests were performed in 4-point bending at room temperature. The fractured surfaces of the samples were investigated by low-power optical microscopy and by high magnification scanning microscopy. Microhardness and fracture toughness were measured with the indentation technique. X-ray diffraction analysis was used to evaluate the crystallographic changes taking place during the mechanical tests.

2 EXPERIMENTAL

2.1 Material

The test bars were supplied by Friedrichsfeld, West Germany, and consisted of commercial Y-TZP material. According to the supplier the flexure strength should be 800 MPa. The corners on the tensile side were chamfered by ABB Cerama, Sweden. The test bars had dimensions b = 4.5 mm width, h = 3.5 mm height and length 50 mm.

2.2 Test equipment

The four-point test jig was built in accordance with US MIL STANDARD 1942/11/ which is expected to form the basis for the coming ISO standard for bend testing [3]. The jig can be constructed with or without independent pivoting of the bearing cylinders. According to the standard, independent pivoting is required only if specimens are as-fired, heat treated of oxidized in such a manner that the specimens are warped or an irregular surface precludes even load application. Since the

test jig is intended for testing of precision machined specimens, it was not constructed with the possibility of independent pivoting.

Loadings were performed in an INSTRON 1341 calibrated servo-hydraulic testing machine. The machine has a 100 kN load cell which can be scaled down to 50 kN. Since only a small part of the working range is utilized during the tests, the calibration was checked with a 2 kN standard cell for each 100 N. Registred error was less than 0.5% in the range concerned. All tests were performed in load control.

Laser technique [4] was used to find out the maximum frequency which could be used during the cyclic fatigue tests. No change in amplitude of the reflected laser beam was observed from 1 Hz up to 25 Hz. This latter frequency was used in all cyclic tests.

The cyclic loadings were all performed with R = 0.1, where

$$R = \frac{\sigma_{mean} - \sigma_a}{\sigma_{mean} + \sigma_a}$$

σ_{mean} is mean applied stress and σ_a is the amplitude of the applied cyclic stress.

The fracture toughness K_{IC} was measured by the Vickers microcrack indentation method using the equation by Evans & Charles [5].

$$K_{IC} = 0{,}16 \cdot H \cdot a^{1/2} \cdot (c/a)^{-3/2}$$

where H is hardness, a is half the length of the diagonal in the indentation and c is the crack radius.

Indentations were obtained with a calibrated Vickers indenter in a Reicherter - Briviskop. The sample was polished to a mirror-like surface with 3 µm diamond-paste. c and a were measured in an optical microscope at 200X magnification. The sample was tested at loads of 100, 200, 300, 400 and 500 Newton in order to determine the load dependence of the fracture toughness.

2.3 Fractography

Fractured surfaces of broken samples were analyzed with low power optical microscopy in order to locate the failure origin. The samples were then gold coated by sputtering and examined by scanning electron microscopy (SEM) in a JEOL 35. Most of the work in the SEM was performed at magnifications between 1000 and 11000 times. It was observed that the gold coating provided enhanced reflectivity of the samples for the optical microscopy, and subsequently all the fractography was performed on gold-coated fracture surfaces.

2.4 Microstructure X-ray investigation

One of the possible strengthening mechanisms in yttria tetragonal zirconia polycrystals is the transformation from the tetragonal metastable phase to a monoclinic phase at the tip of a propagating crack [6, 7]. Since the volume of the monoclinic phase is 5% higher then of the tetragonal phase, a local compression is created, which increases the crack resistance. Other strengthening mechanisms in transformation-toughened zirconia materials are generation of microcracks [8, 9] and ferroelastic domain twinning of tetragonal grains [10]. Both the amount of transformation and the degree of twinning can be calculated from x-ray profiles [11].

X-ray diffraction profiles were obtained on fracture surfaces from samples broken in different ways and on side surfaces on both fatigued and on as-received test bars.

3 RESULTS

3.1 Cyclic fatigue data

Test bars were cyclically loaded at four stress levels σ_{max}, where $\sigma_{max} = \sigma_{mean} + \sigma_a$; 400, 450, 500 and 550 MPa.

Six samples were tested at each stress level. The tests were terminated after 2×10^6 cycles if the test bar did not fail. In addition, one test bar was cycled at 400 MPa up to 10^7 cycles without failure.

All broken samples failed between the inner rollers, in gen- eral not at the contact points between the rollers and the sample.

A graphical evaluation of the test data from the three highest stress levels is presented in fig. 1, 2 and 3 in ANNEX. A fit to a log-normal distribution is acceptable at all three levels. Mean values of log N and estimated standard deviations are shown in the diagrams.

An evaluation of a possible fatigue limit and the standard deviation were graphically determined [12] from the data for 450 MPa and 400 MPa as shown in diagram 4 in ANNEX.

Figure 1 shows the S-N curve at room temperature for Y-TZP. Although the spread in data is quite large, the results show a strong decrease in the number of cycles to failure with increasing maximum stress level. The results also indicate a possible fatigue limit at about 435 MPa. As can be seen from the diagram the samples cycled at the highest stress level - 550 MPa - on average lasted for $2 \cdot 10^3$ cycles.

3.2 Static and monotonic loading

It could be argued that the behaviour demonstrated in figure 1 is not cyclically induced, but simply due to subcritical environmentally-assisted cracking processes at maximum load. A few samples were statically loaded at 500 MPa. All statically loaded samples failed after some time, but the times to failure were in all cases longer than the time to failure under cyclic loading at the same maximum cyclic load level.

According to the manufacturer, the flexure strength of the material should be 800 MPa. Six test bars were monotonically loaded to failure at a crosshead rate of 0.5 mm/min. The mean value obtained was 639 MPa, with a standard deviation of 18 MPa. All samples failed very close to the contact point between one of the inner rollers and the test bar.

3.3 Monotonic loading of fatigued samples

Five samples which were still intact after $2 \cdot 10^6$ cycles at 400 MPa were monotonically loaded to failure. Three of these had been removed from the test jig after cycling. The observed flexure strength was about 500 MPa and the failure for these bars occured close to one of the inner rollers.

The other two samples were loaded to failure without having been removed from the test jig after cycling. These test bars showed the highest strength of all samples tested - one had a flexure strength close to 800 MPa. For these two samples the failure occured between the inner rollers.

3.4 Fracture toughness

Twenty values for a and c were measured for each load F. The results of the measurements of Vickers hardness and fracture toughness are shown in figs. 2 and 3.

3.5 Fractography

Most of the tested samples were investigated with both low-power optical microscopy and high magnification scanning electron microscopy.

The main effort has been to try to observe microscopic differences between samples deformed in the following modes:

A; Cyclically loaded to failure

B; Monotonically loaded to failure

C; Statically loaded to failure

D; Cyclically loaded 10^7 or $2 \cdot 10^6$ cycles without failure and then monotonically loaded to failure.

Representative micrographs are shown in figures 4 to 8.

A; Figures 4a, b, c are obtained on the fracture surface of a sample cyclically loaded to failure at 450 MPa, N = $7.4 \cdot 10^5$ cycles.

B; Figures 5a, b, c are obtained at corresponding locations on a sample monotonically loaded to failure at 625 MPa.

In both cases the failure of origin was clearly identified on the tensile surface between the chamfered corners. The main difference between the two samples can be observed in the vicinity of the origin of failure in a semicircular area with a radius of about 50 µm. For the fatigued sample, the fatigue zone seems to be intergranular and contains a number of microcracks. Outside the fatigued zone, the fracture seems to be transgranular with few cracks.

The difference in surface appearance between the areas outside and inside the fatigued zone is clearly demonstrated in figures 6a and b. Figure a is obtained 50 µm from the failure of origin while figure b is obtained 200 µm from the failure of origin on the same sample.

In the fracture surface of the monotonically loaded sample, the fracture seems to be transgranular and few microcracks are observed. No semicircular area near the failure of origin can be seen.

C; Micrographs obtained on fracture surface from a sample statically loaded to failure at 500 MPa are shown in figure 7. The fracture is presumed to be mainly transgranular.

D; A sample which did not fail after 10^7 cycles at 400 MPa was loaded to failure. The flexure strength obtained was 700 MPa. A micrograph from the fracture surface is shown in figure 8. As can be seen from the micrograph, the fracture is a mixture of transgranular and intergranular fracture.

3.6 X-ray diffraction data

X-ray diffraction profiles obtained on both deformed and undeformed samples are shown in figure 9. The volume fraction of the monoclinic phase can be determined [11] from the area under the peaks $(11\bar{1})_m$, $(111)_m$ and $(111)_t$. Calculations indicate 5% monoclinic phase on all side surfaces, both on cycled and undeformed samples. The amount of monoclinic phase in the fractured surfaces was 25 - 30% on all broken samples, independent of in what way the samples had been deformed.

4 DISCUSSION

Cyclic fatigue data have now been reported for a number of monolithic ceramics. In a recent review paper Grathwohl and Liu [7] have presented results for several materials. They also reported experimental results on strengthening effects by cycling of zirconia-alumina and suggested this to be an effect of the transformation from tetragonal to monoclinic phase in the crack tip during cycling.

Most of the published work on cyclic fatigue of zirconia materials has been presented by Ritchie et al [2]. They have concentrated on Mg-PSZ ceramics and have clearly demonstrated the existence of true cyclic fatigue phenomena in these ceramics.

In the present report results from cyclic bending of yttria tetragonal zirconia polycrystals are presented. As can be seen from the S-N curve in figure 1, the lifetime decreases with increasing maximum cyclic load. An appearent fatigue limit at $2 \cdot 10^6$ cycles was estimated to be 65% of the flexure strength in 4-point bending.

Very high values of both flexure strength and fracture toughness have been reported for tetragonal zirconia polycrystals [13]. The values found in the present investigation are much lower. The reason for this is not understood, but could to some extent be explained by the fact that the samples used were tested as received without any special surface treatment.

Almost all published reports on cyclic fatigue in ceramics have concentrated on the mechanical behaviour. No systematic investigations have been published in which attemps have been made to correlate the morphology of fractured surfaces with the mode of fracture.

In the present report, the purpose has been to investigate fractured surfaces at high magnifications in the electron scanning microscope, in order to find out as much as possible about the possible processes which could explain the observed fatigue behaviour.

All fractographic studies show transgranular fracture exept for fatigued samples, in which a small area in the vicinity of the origin of fracture is presumed to be intergranular. The suggested mechanism for the cyclic fatigue is the following.

The fracture starts from a defect, which in this study always has been situated in the tensile surface of the test bar. During cyclic loading intergranular cracks propagate out from the defect and a weaker area extends into the material. After a number of cycles, the area has reached a critical size and the test bar fails in a catastrophic manner in accordance with the Griffith law. According to the micrographs in figure 6, the size of the fatigued zone for that sample is of the order of 100 µm.

The diameter of the fatigued zone for other samples has also been observed to be about 100 µm. The value of fracture toughness for this material, as determined by indentation technique measurement, is about 5 $MN \cdot m^{-3/2}$. With this value in the Griffith equation $\sigma_{fracture}$ is found to be 500 MPa, which is close to the flexure strength in view of the uncertainty in the measured fracture toughness.

For σ_{max} = 450 MPa, the number of cycles to failure is 10^5 as shown in figure 1. For a fatigued zone with a radius of 50 µm this means that each cycle in general should propagate the subcritical crack a distance of about 5 Å. That means that each cycle in general breaks bonds between a few atoms in each crack.

According to Grathwohl et al [7], the observed increase in flexure strength after cycling could be caused by an increase of the monoclinic phase in the material during the cycling. This can probably not be the whole truth, since in the present report, the amount of monoclinic phase in the fracture surfaces was found to be the same for both cycled and monotonically loaded samples.

5 CONCLUSIONS

It has been demonstrated that cyclic fatigue may cause damage to yttria tetragonal zirconia polycrystals.

Scanning electron fractographs indicate intergranular fracture in a fatigue zone in the vicinity of the origin of failure for fatigued specimens. The fracture area outside this zone seems to be transgranular and shows the same morphology as monotonically fractured samples.

The mechanisms for fatigue failure is dependent on the number of cycles and to a less extent time dependent.

X-ray diffraction analysis on fracture surfaces shows the same degree of transformation from tetragonal to monoclinic phase, independent of the way of loading to failure.

The role of cyclic stress is supposed to be opening and closing of intergranular micro-cracks and be reactivation of arrested cracks by going around or across the crystals by subsequent cyclic loadings.

6 ACKNOWLEDGEMENTS

The author wishes to thank Hans Andersson and Robert Pompe for many valuable discussions and Håkan Torstensson and Thomas Gevert for encouraging support. The author also would like to thank M.E.S. Ali at RISO National Laboratory, Roskilde for performing the X-ray diffraction analyses.

7 REFERENCES

[1] A.G. Evans, "Fatigue in Ceramics," Int. J Fract., 16 485 - 98 (1980.

[2] R.H. Dauskardt, D.B. Marshall, and R.O. Ritchie, "Cyclic Fatigue-Crack Propagation in Mg-PSZ Ceramics". J. Am. Ceram. Soc., 73 (4) 893 - 209 (1990).

[3] "Flexure Strength of High Performance Ceramics at Ambient Temperature", US MIL - STD - 1942 (MR), (1983).

[4] L. Carlsson, "Cyclic Fatigue of Hot - Isostatic - Pressed Silicon Nitride", SP Report 1989:43 (1989).

[5] A.G. Evans and E.A. Charles, "Fracture Toughness Determination by Indentation", J. Am. Ceram. Soc., 59 [7-8] 371 - 372 (1976).

[6] R.C. Garvie, R.H.J. Hannink and R.T. Pascoe, "Ceramic Steel", 258 703 - 704 (1975).

[7] G. Grathwohl and T. Liu, "Strengthening of Zirconia-Aluminia During Cyclic Fatigue Testing", J. Am. Ceram. Soc., 72 (10) 1988 - 90 (1989).

[8] J.W. Hutchinson, "Crack Tip Shielding by Micro-Cracking in Brittle Solids," Acta Metall., 35 (7) 1605 - 19 (1987).

[9] S. Suresh, and J.R Brockenbrough, "Theory and Experiments of Fracture in Cyclic Compression: Single Phase Ceramics, Transforming Ceramics and Ceramic Composites," Acta Metall 36 (6) 1455 - 70 (1988).

[10] A.V. Virkar, and R.L.K. Matsumoto, "Ferroelastic Domain Switching as a Toughening Mechanism in Tetragonal Zirconia", J.Am. Ceram. Soc., 69 (10) C-224 - C226 (1986).

[11] H. Toraya, M. Yoshimura, and S. Sömiya, "Quantitative Analysis of Monoclinic-Stabilized Cubic ZrO_2 Systems by X-Ray Diffraction", J.Am. Ceram. Soc., 67 (6) C183 - C184 (1984).

[12] R.E. Little, and E.H. Jebe, "Statistical Design of Fatigue Experiments", Applied Science Publishers Ltd., London, 1975.

[13] D.J. Green, R.H.J. Hannik, and M.V. Swain, "Transformation Toughening of Ceramics", C.R.C. Press, Inc., Florida, 1989.

8 FIGURES

Fig. 1 S-N curve for yttria tetragonal zirconia polycrystals.

Fig. 2 Fracture toughness as a function of applied load.

Fig. 3 Vickers hardness as a function of applied load.

Fig. 4 Micrographs obtained on a fracture surface of a sample cyclically loaded to failure at 450 MPa, $N = 7,4 \times 10^5$.

Fig. 5 Micrographs obtained at corresponding locations on a sample monotonically loaded to failure.

Fig. 6 Micrographs obtained at differrent locations on a specimen cyclically loaded to failure.

a) 50 µm from origin of failure
b) 200 µm from origin of failure.

Fig. 7 Micrograph obtained on a fracture surface of a sample statically loaded to failure.

Fig. 8 Micrograph obtained at corresponding location as in Fig. 7 from a sample cyclically loaded 10^7 cycles, then monotonically loaded to failure.

Fig. 9 X-ray diffraction profiles obtained on deformed and undeformed samples.

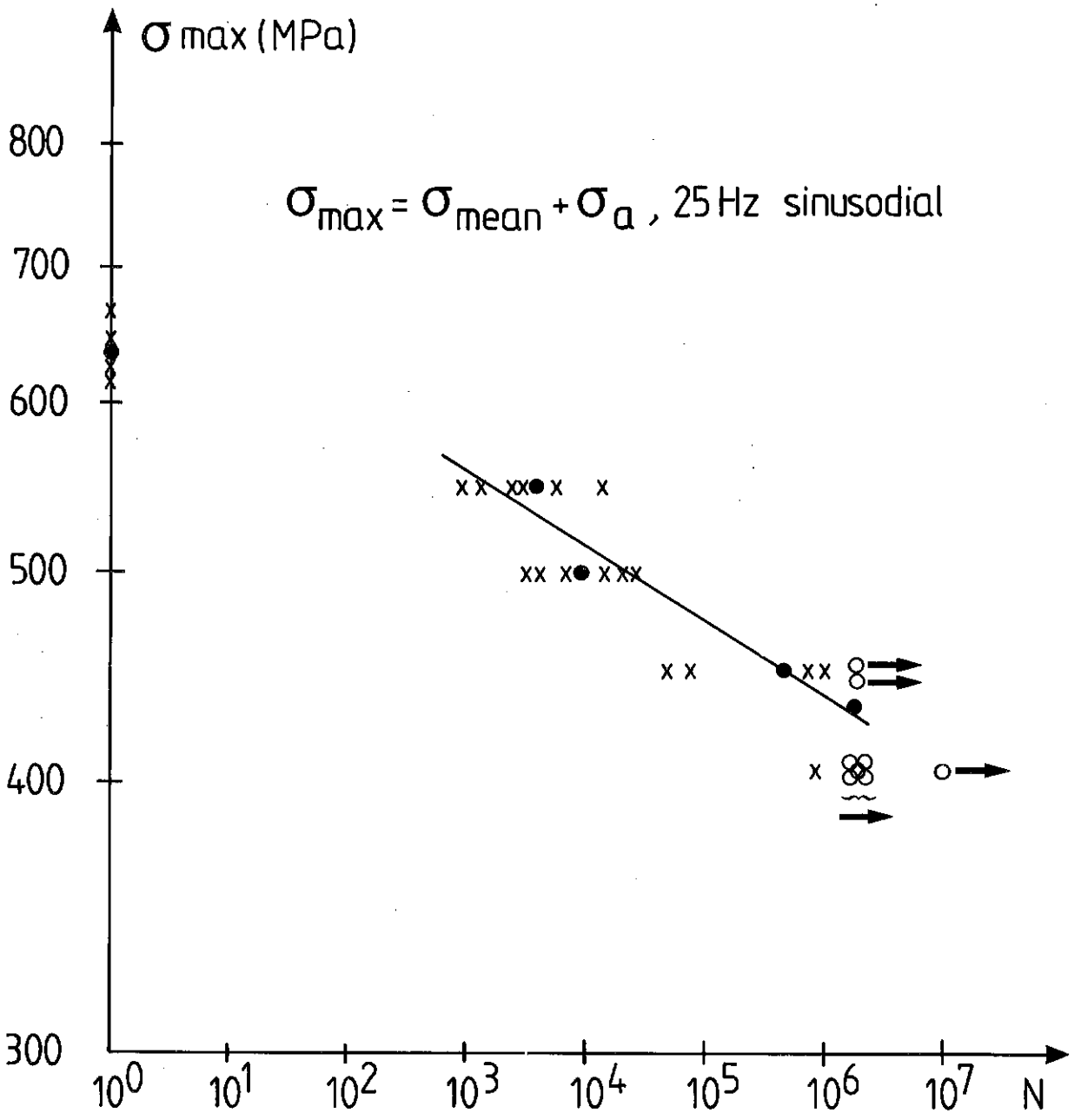

Fig. 1 S-N curve for yttria tetragonal zirconia polycrystals.

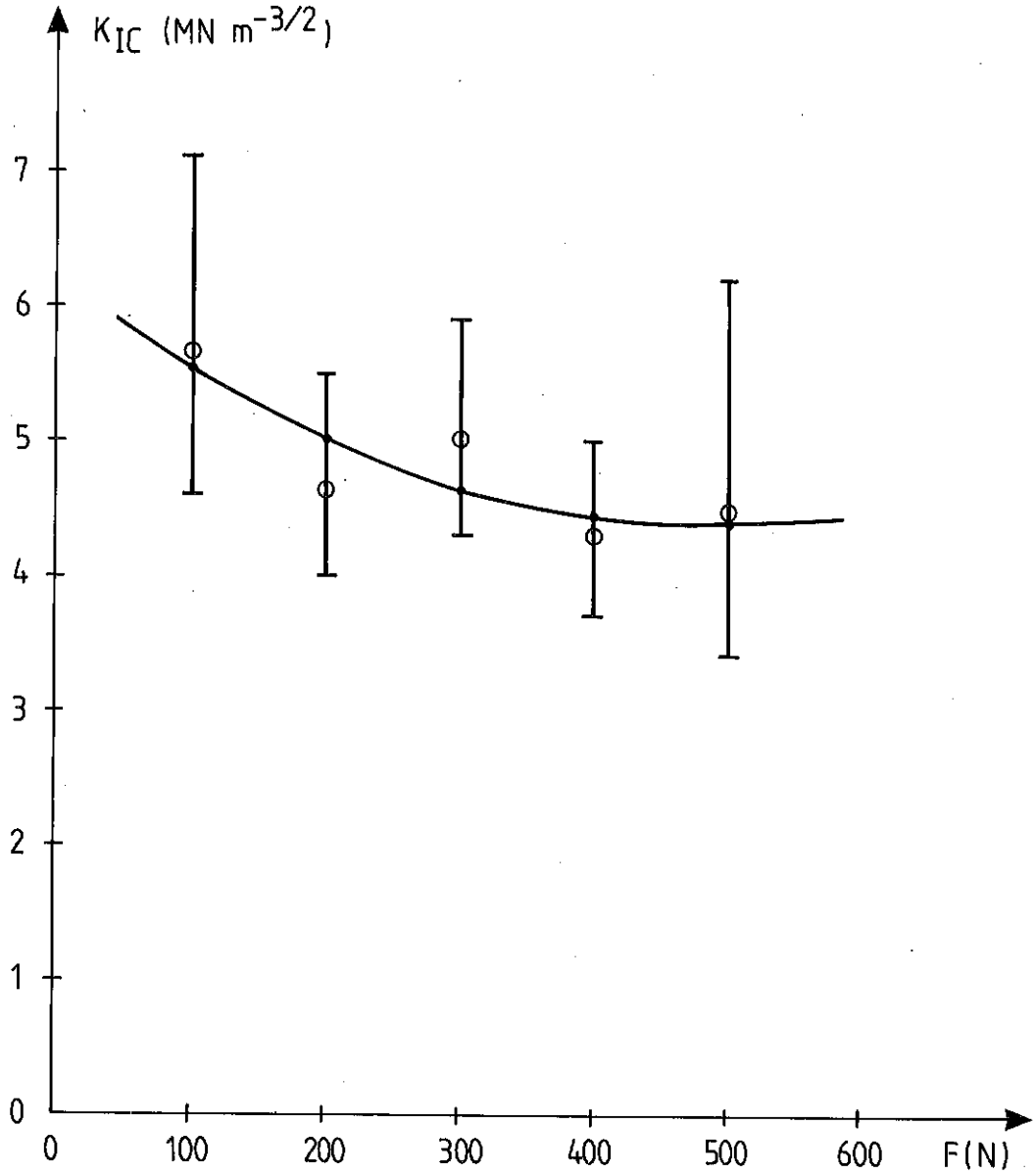

Fig. 2 Fracture toughness as a function of applied load.

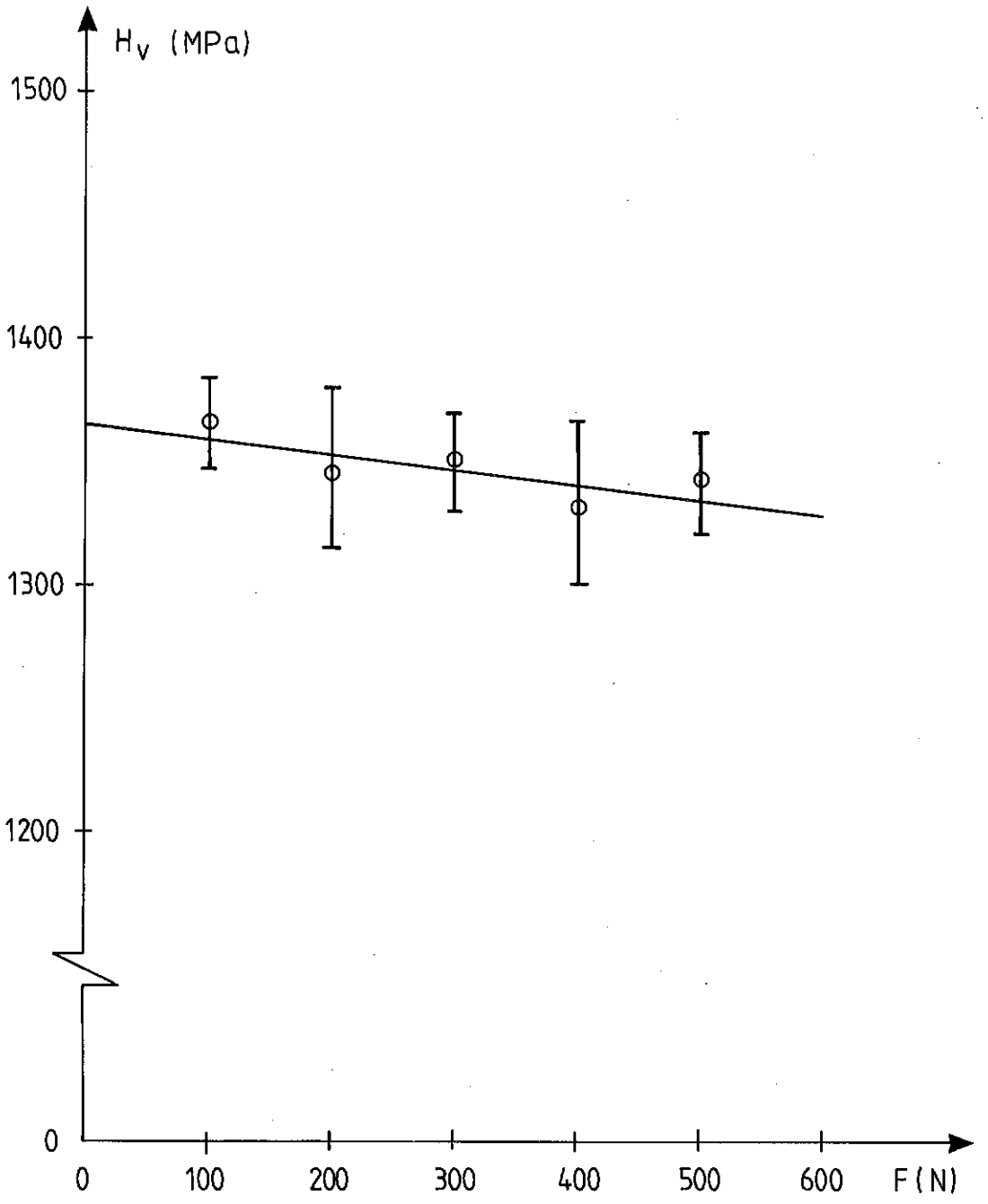

Fig. 3 Vickers hardness as a function of applied load.

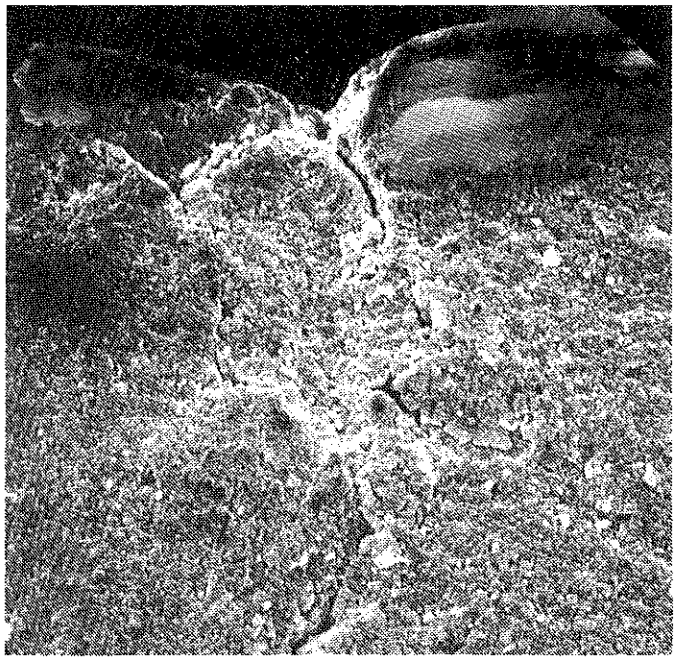

a)

25 µm

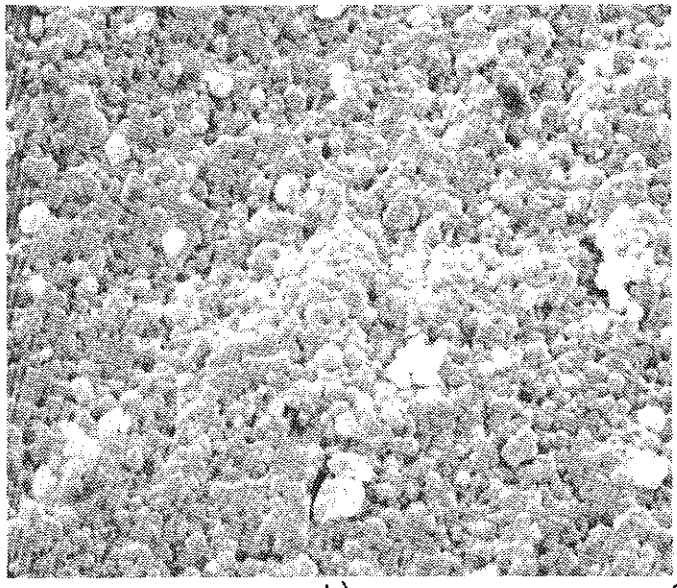

b)

6 µm

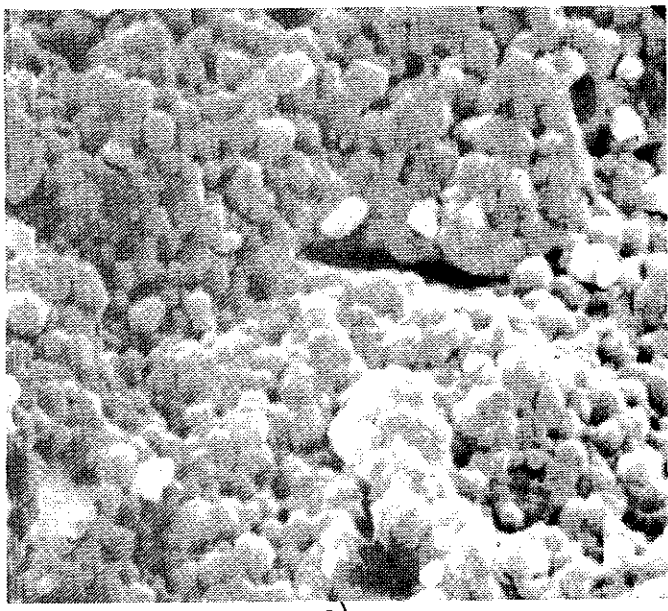

c)

3 µm

Fig. 4 Micrographs obtained on a fracture surface at a sample cyclically loaded to failure at 450 MPa, N = 7,4 x 10^5 cycles.

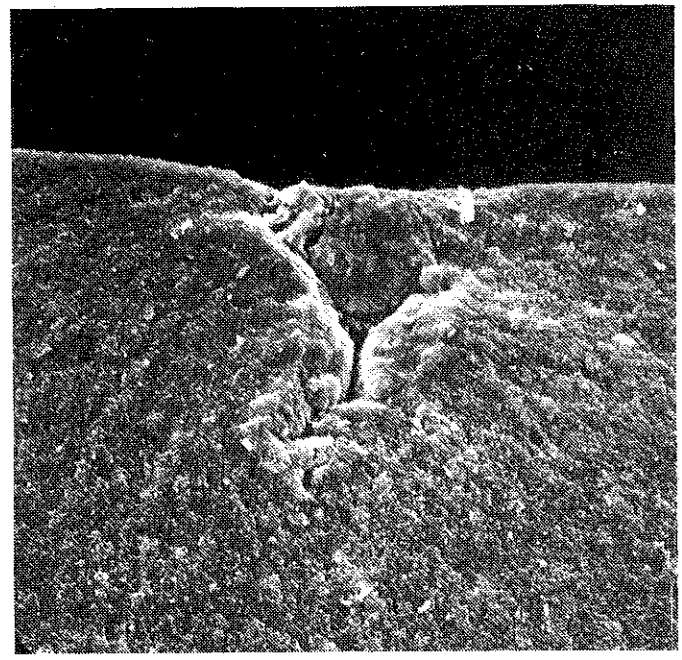

a)

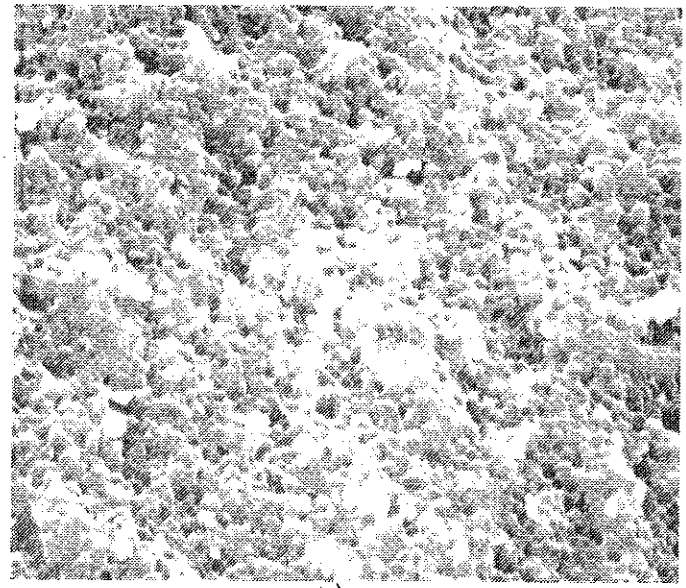

b)

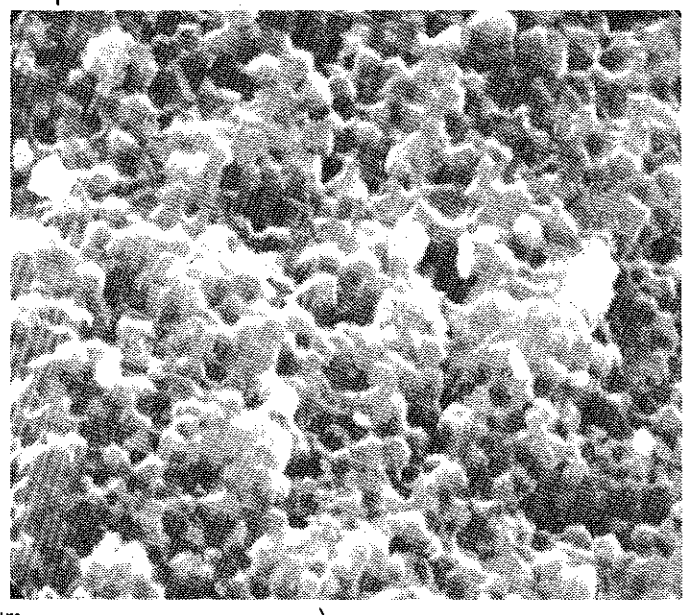

c)

Fig. 5 Micrographs obtained at corresponding locations on a sample monotonically loaded to failure.

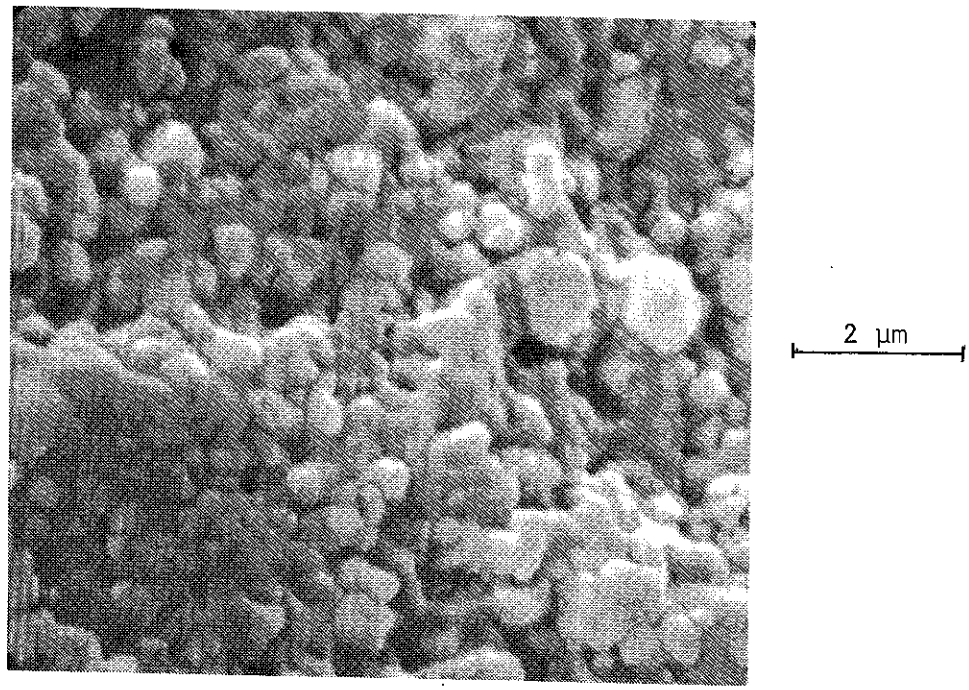

(a)

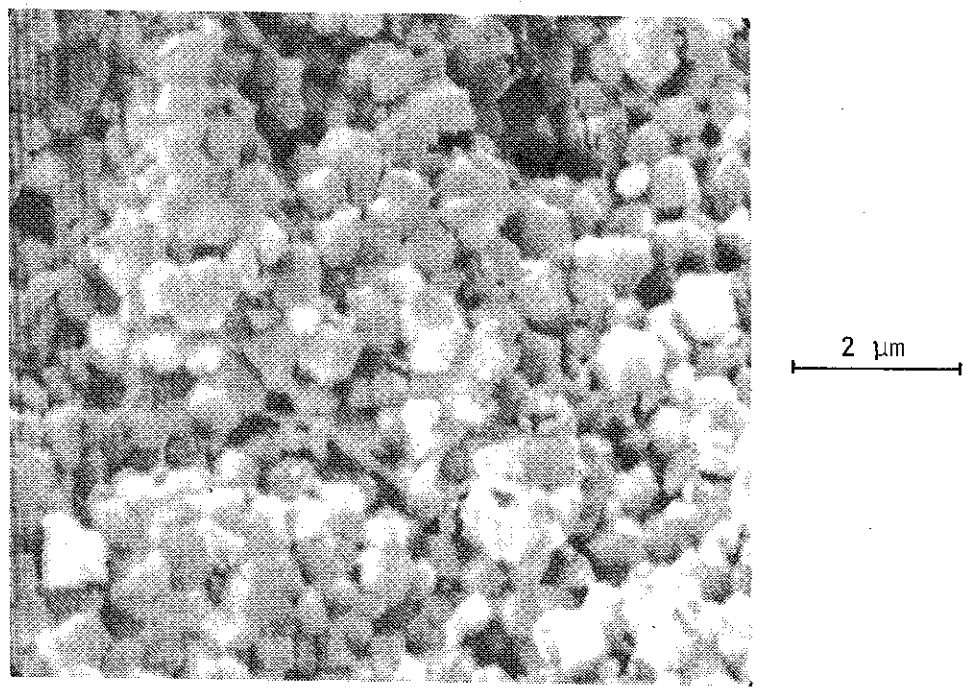

(b)

Fig. 6 Micrographs obtained at different locations on a specimen cyclically loaded to failure.

a) 50 μm from origin of failure.

b) 200 μm from origin of failure.

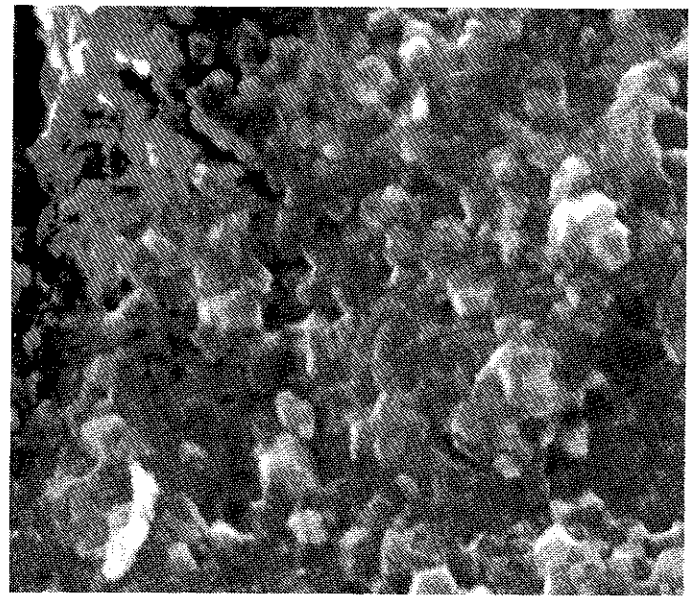

Fig. 7 Micrograph obtained on a fracture surface of a sample statically loaded to failure.

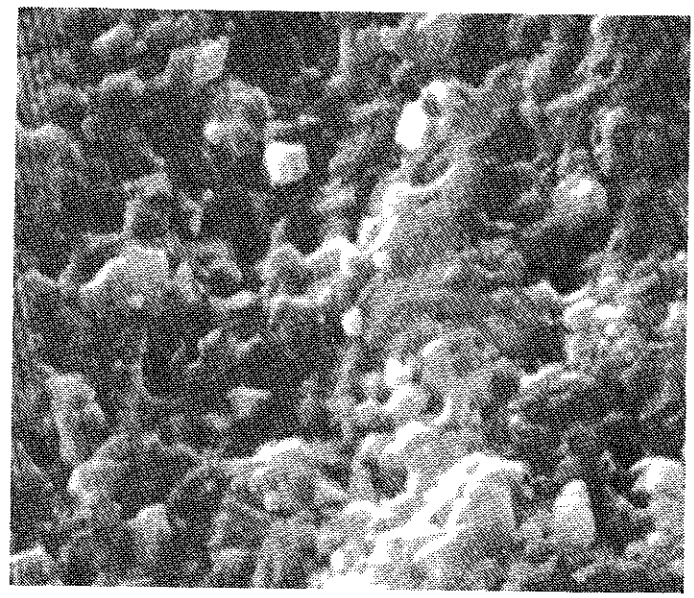

Fig. 8 Micrograph obtained at corresponding location as in Fig. 7 from a sample cyclically loaded 10^7 cycles, then monotonically loaded to failure.

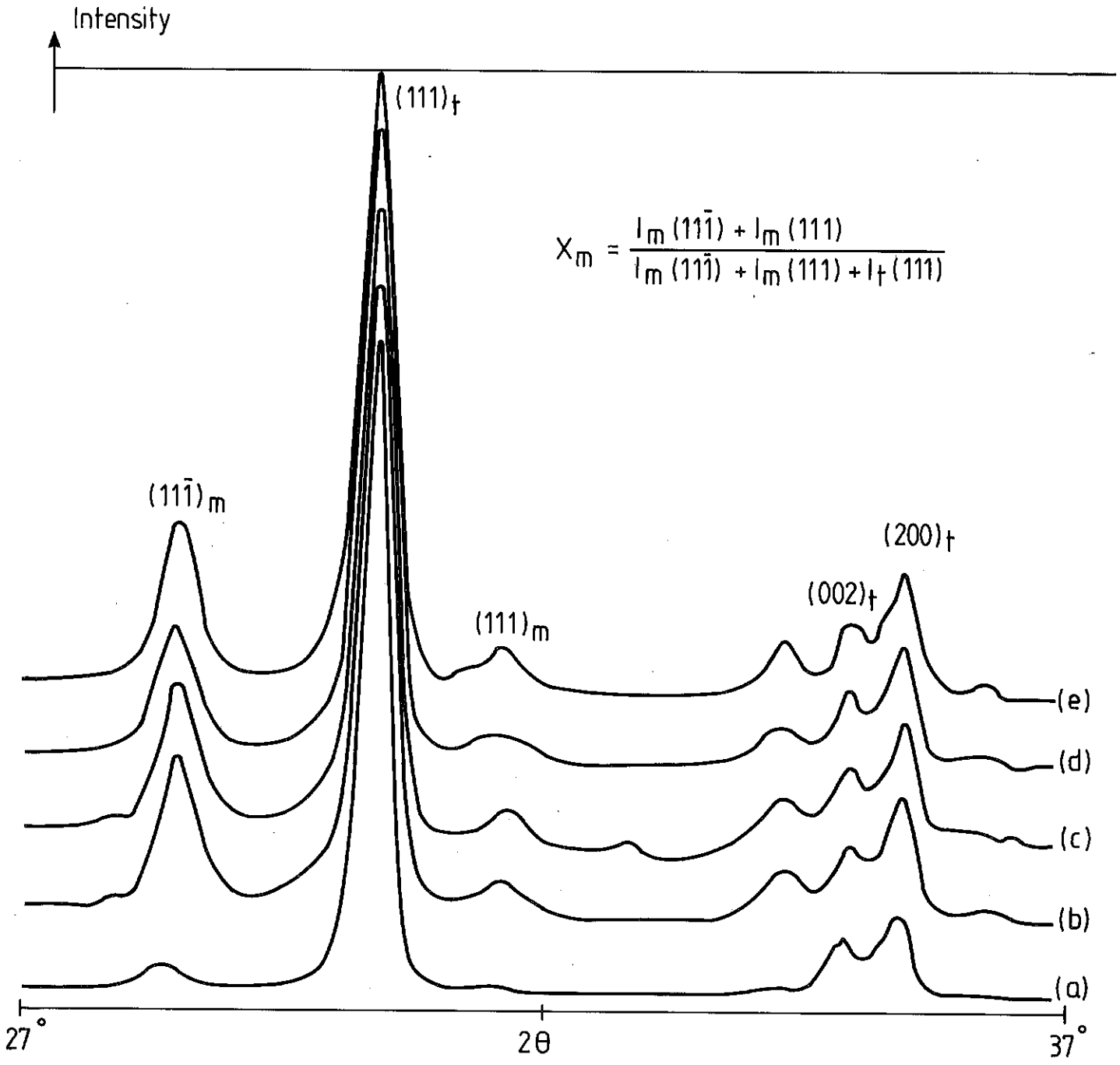

X-ray diffraction profiles obtained on:

(a) sides of undeformed or deformed samples

(b) fracture surface $\sigma_{max} = 550$ MPa $N = 1.3 \times 10^4$ cycles

(c) —"— —"— monotonically loaded to fracture $\sigma_{fr} = 645$ MPa

(d) —"— —"— statically loaded to failure at 500 MPa 3.5 hour

(e) —"— —"— did not failure under cycling at 400 MPa 10^7 cycles, loaded to failure, $\sigma_{fr} = 700$ MPa

Fig. 9 X-ray diffraction profiles obtained on deformed and undeformed samples.

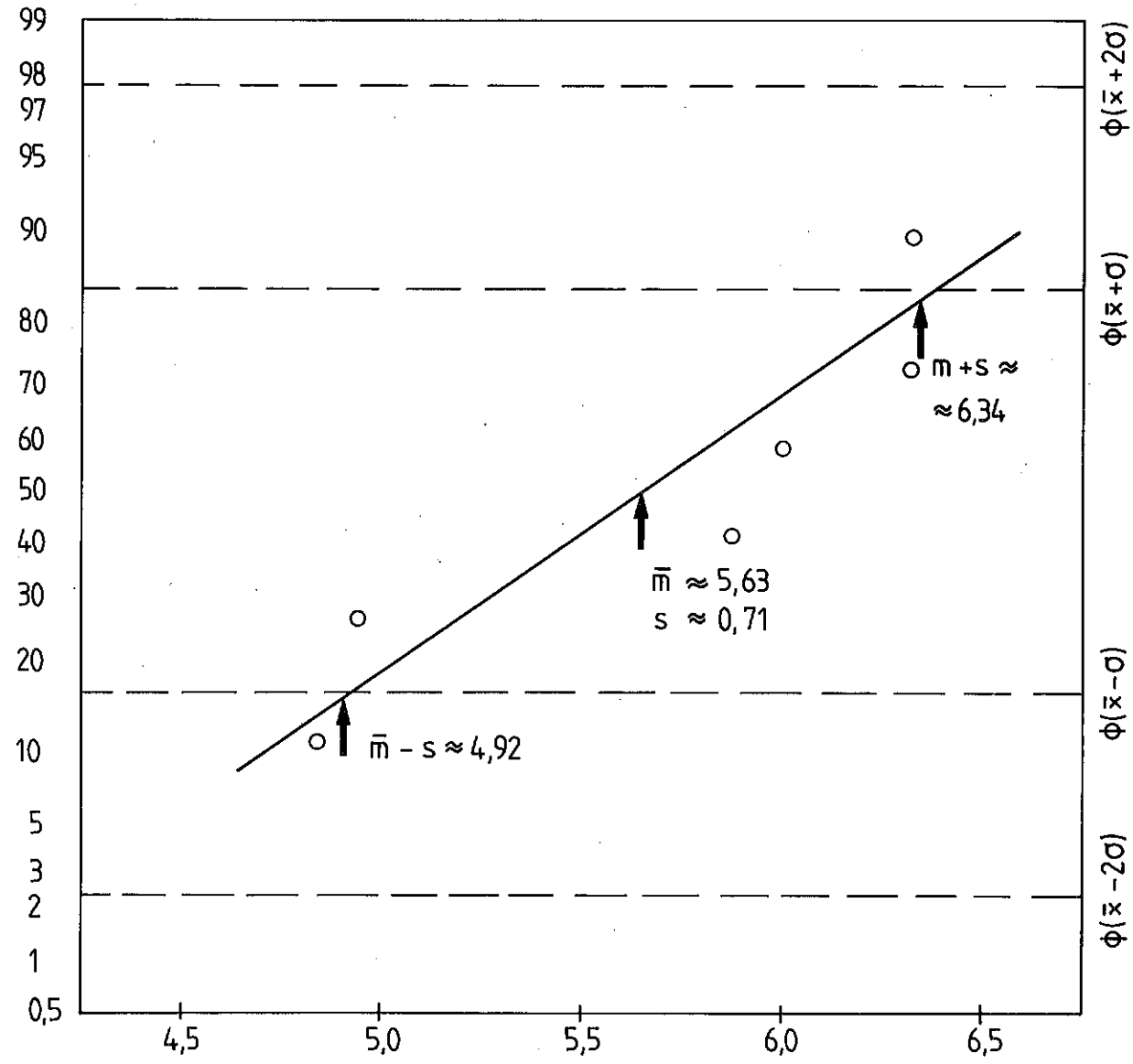

ANNEX Fig. 1 σ_{max} 450 MPa.

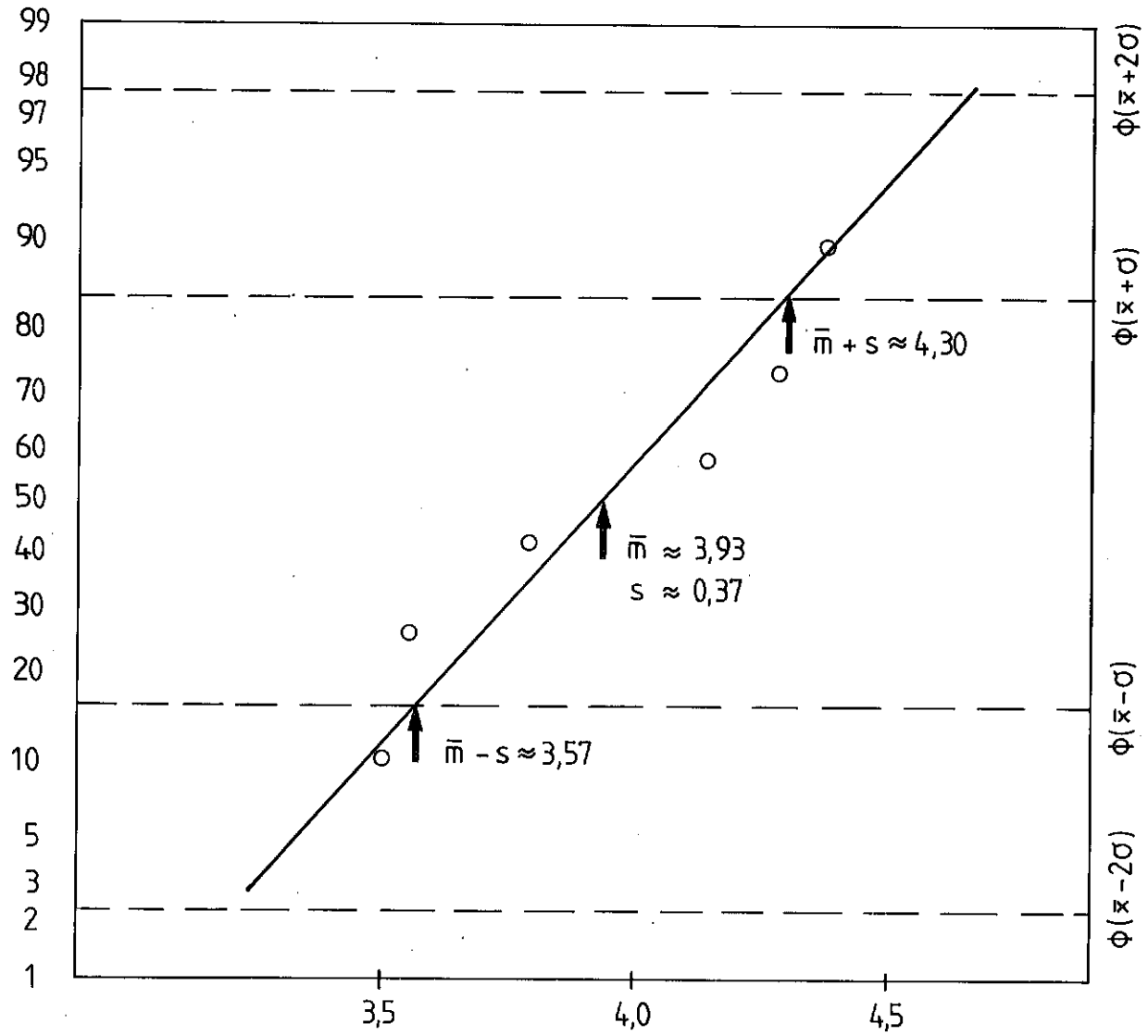

ANNEX Fig. 2 σ_{max} 500 MPa.

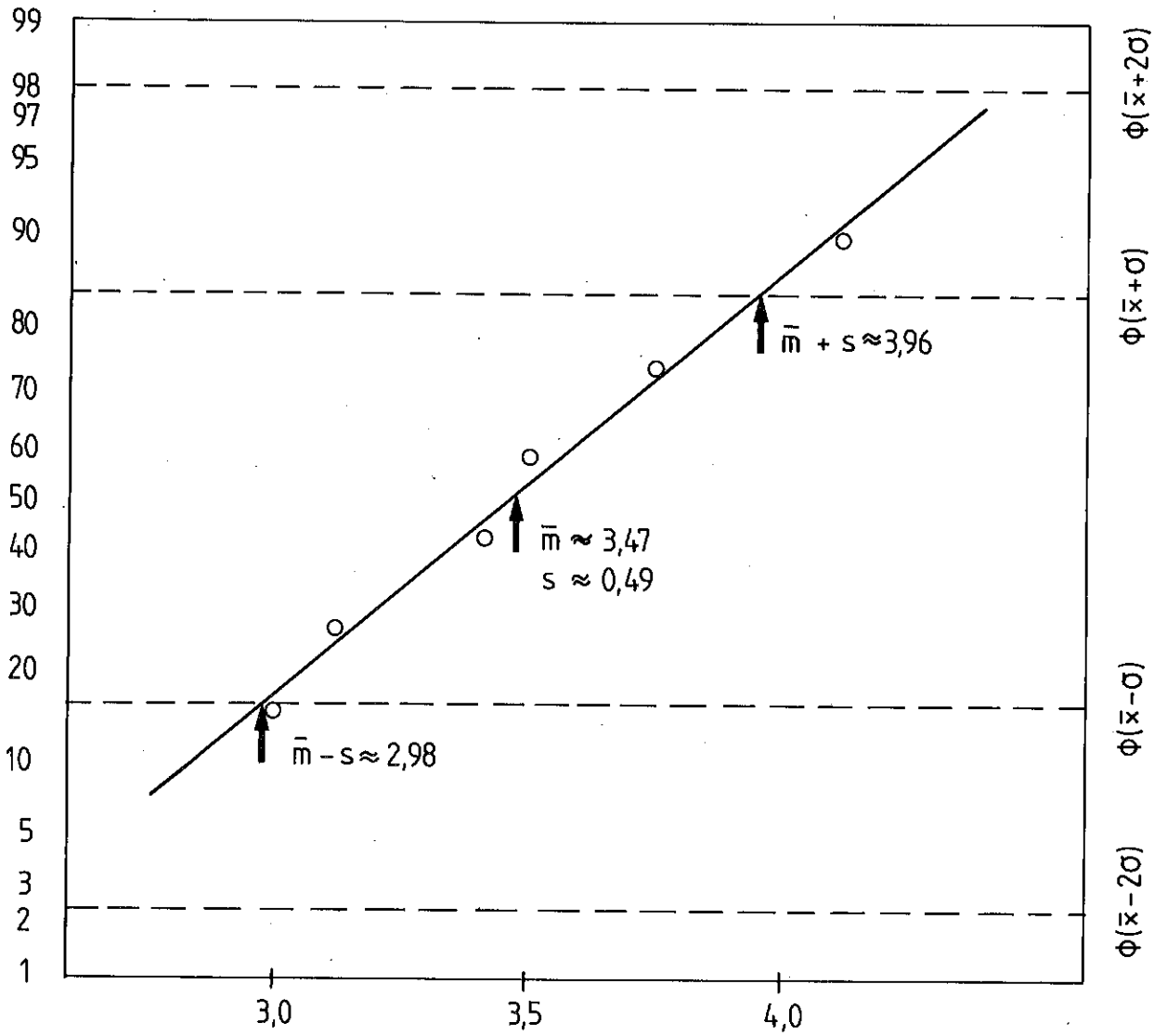

ANNEX Fig. 3 σ_{max} 550 MPa.

$\sigma 1 = 400$ MPa $N1 = 6$, $R1 = 5$

$\sigma 2 = 450$ MPa $N2 = 6$, $R2 = 2$

$P1 = 0{,}167$

$P2 = 0{,}667$

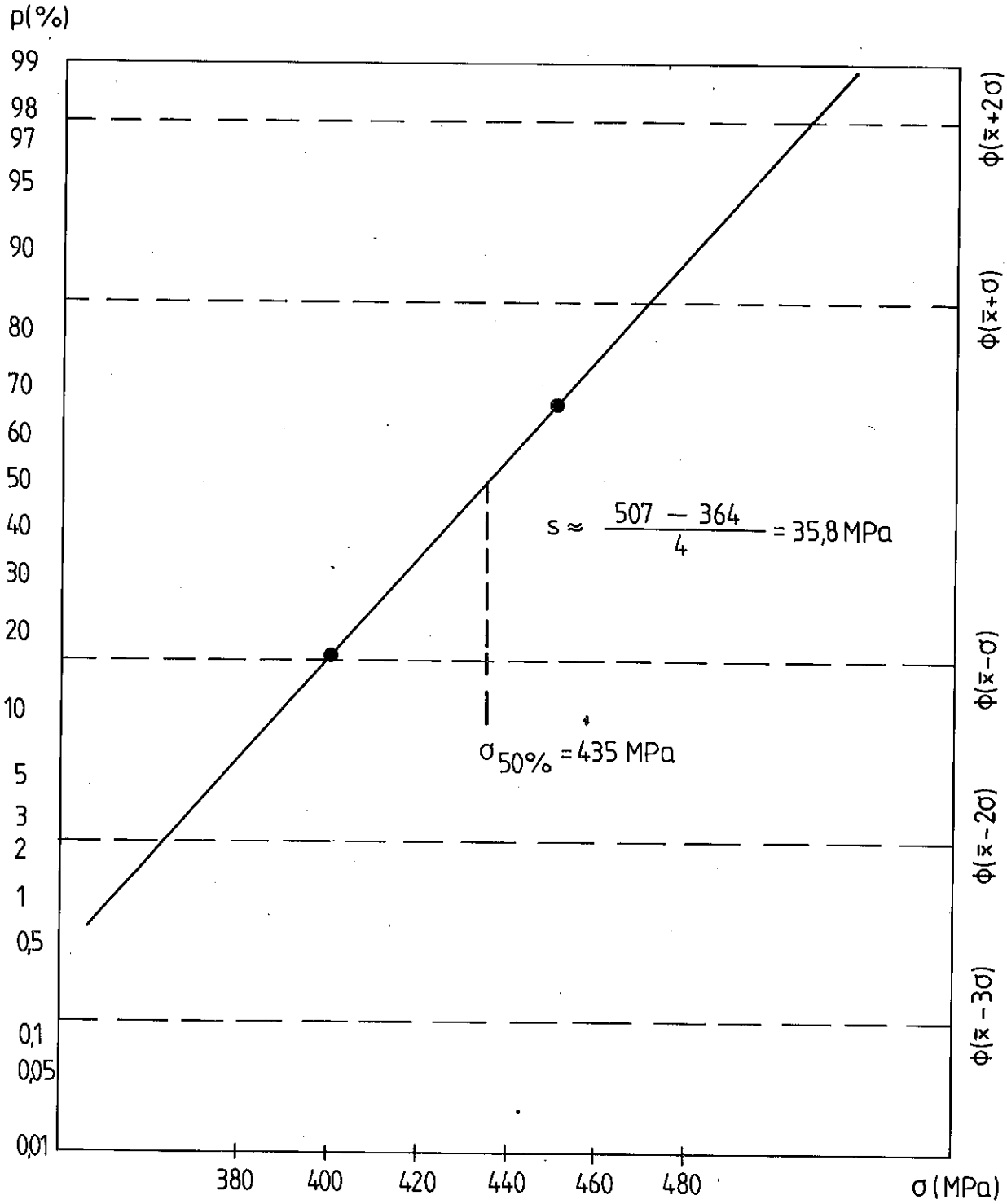

ANNEX Fig. 4 Estimation of a possible fatigue limit by the two-point method.